Observational Study

Medicine®

OPEN

# Differentiation of testicular seminoma and nonseminomatous germ cell tumor on magnetic resonance imaging

Renwei Liu, MS[a,*], Zhengxian Lei, MS[b], Aibo Li, MS[a], Yixiang Jiang, MS[a], Jiayin Ji, MS[a]

**Abstract**

Magnetic resonance imaging (MRI) has excellent soft tissue resolution, as well as multidirectional and multisequence scanning technology, making it an important supplementary method in the diagnosis of testicular tumor.

To explore the utility of preoperative MRI for the differential diagnosis of testicular seminoma and nonseminomatous germ cell tumors (NSGCTs).

The medical records from 39 patients with testicular tumors that were examined preoperatively with MRI and treated with urologic surgery at our institution between January 2015 and March 2019 were retrospectively reviewed. Testicular tumors were confirmed by pathology and classified as seminoma (n = 20) or NSGCT (n = 19). Two radiologists analyzed the testicular tumors on preoperative MRI for morphology: multiple nodules or a single mass; presence/absence of a capsule; signal compared to the normal contralateral testicle (isointense, hypointense, hyperintense, or mixed); enhancement; septa; and hemorrhagic or cystic degeneration. Characteristics of seminomas and NSGCT were compared using the Chi-square or Fischer exact test.

MRI showed that the majority (95%; 19/20) of seminomas were nodular. There were significant differences in the presence/absence of a capsule ($P = .001$), T1-weighted imaging (T1WI) signal intensity ($P = .047$), T2-weighted imaging (T2WI) signal intensity ($P < .001$), septa ($P < .001$), and hemorrhagic or cystic degeneration ($P < .001$) between seminomas and NSGCT.

Seminomas were more likely to have no capsule, isointensity on T1WI, hypointensity on T2WI, and had narrow obviously enhanced fibrovascular septa without hemorrhagic or cystic degeneration; NSGCT was more likely to have a capsule, a mainly mixed signal on T1WI and T2WI, most of them had no fibrovascular septa, and hemorrhagic or cystic degeneration was common in malignant NSGCT.

This study suggests that preoperative MRI can distinguish seminoma from NSGCT. We propose that preoperative MRI of the scrotum is an effective technique that should be widely adopted for the management of scrotal disease.

**Abbreviations:** AFP = alpha fetoprotein, CT = computed tomography, GCT = germ cell tumor, β-HCG = human chorionic gonadotropin, MGCT = mixed germ cell tumor, MRI = magnetic resonance imaging, NSGCT = nonseminomatous germ cell tumor, T1WI = T1-weighted imaging, T2WI = T2-weighted imaging, TEC = testicular epidermoid cyst, US = ultrasonography.

**Keywords:** magnetic resonance imaging, NSGCT, seminoma, testicular tumors

## 1. Introduction

Germ cell tumors (GCTs) account for an estimated 98% of testicular tumors, while seminomas account for more than 55% of GCTs.[1] Testicular tumors are usually diagnosed by ultrasonography (US); however, US may not differentiate benign from malignant lesions or accurately predict tumor size.[2,3] Magnetic resonance imaging (MRI) has excellent soft tissue resolution, as well as multidirectional and multisequence scanning technology, making it an important supplementary method in the diagnosis of scrotal diseases,[4] and a useful tool for problem-solving.[5]

MRI is accurate for preoperative differentiation of benign from malignant testicular tumors, local staging of testicular malignant masses, and for guiding clinical decision making. Currently, treatment of benign testicular tumors adopts an organ-sparing policy, and the tumor is enucleated. Radical inguinal orchiectomy is performed in patients with malignant tumors, followed by radiotherapy or chemotherapy. Postoperatively, MRI is effective for detecting residual tumor, local recurrence, and distant metastasis. The objective of this study was to explore the utility of preoperative MRI for the differential diagnosis of testicular seminoma and nonseminomatous germ cell tumor (NSGCT).

*Editor: Giuseppe Lucarelli.*

*Consent for publication: Informed written consent was obtained from the patient's guardians for publication of this case report and accompanying images.*

*The authors have no conflicts of interest to disclose.*

*[a] Urogenital System Group, Department of Radiology, People's Hospital of Long Hua District, [b] Department of Radiology, The University of Hong Kong, Shenzhen Hospital, Shenzhen, China.*

*[*] Correspondence: Renwei Liu, Department of Radiology, People's Hospital of Long Hua District, No. 38 Jinglongjianshe Road, Shenzhen 518109, China (e-mail: lhhospital@sina.com).*



*How to cite this article: Liu R, Lei Z, Li A, Jiang Y, Ji J. Differentiation of testicular seminoma and nonseminomatous germ cell tumor on magnetic resonance imaging. Medicine 2019;98:45(e17937).*

*Received: 5 July 2019 / Received in final form: 29 September 2019 / Accepted: 14 October 2019*

*http://dx.doi.org/10.1097/MD.0000000000017937*

## 2. Materials and methods

### 2.1. Patients

The medical records of patients with testicular tumors that were examined preoperatively with MRI and treated with urologic surgery at our institution between January 2015 and March 2019 were retrospectively reviewed. Inclusion criteria were: clinical presentation of a painless scrotal swelling requiring MRI examination; and testicular tumors confirmed by pathology, including immunohistochemistry for S100, CD30, α-inhibin, CK, Ki67, CD117, and SALL4. Exclusion criteria were: primary tumors in other parts of the body; recent history of testicular trauma; clinical emergency, suspicious testicular torsion; or recent history of systemic infection.

The following information was recorded: clinical manifestations, laboratory results, imaging data, treatments options, and pathological diagnosis. Preoperative MRI was compared with surgical and pathologic findings.

### 2.2. Preoperative MRI examination

The patient lay on his back. The testicles and scrotum were elevated and supported with a raised towel. MRI was performed with a Philips Ingenia 3.0T scanner using the protocol outlined in Table 1. Contrast enhancement MRI used intravenous gadolinium-diethylenetriaminepentaacetate (0.2 mmol/kg, current speed 2.0 mL/second).

### 2.3. Image analysis and judgment criteria

Two radiologists with 19 and 22 years experience diagnosing abdominal and pelvic masses analyzed the testicular tumors on preoperative MRI for morphology: multiple nodules or a single mass; presence/absence of a capsule; signal compared to the contralateral normal testis, defined as a isointense, hypointense, hyperintense, or mixed; enhancement, defined as mild, medium, significant, uneven, or annular; intralesional septa; and hemorrhagic or cystic degeneration. Characteristics of seminomas and NSGCT on preoperative MRI were compared using the Chi-square or Fischer exact test. $P < .05$ was considered statistically significant.

### 2.4. Ethics statement

The institutional review board of the People's Hospital of Long Hua District approved this study and waived the need for informed consent based on the retrospective study design.

## 3. Results

This study included 39 cases of testicular tumor in patients with a mean age of 39.4 years (range, 12–56 years), mean height of 1.68 m, mean weight of 69.0 kg, and mean body mass index of 24.44 kg/m$^2$. Pathology showed that 20 tumors were seminomas and 19 tumors were NSGCT. MRI showed that the majority (95%; 19/20) of seminomas were nodular (Fig. 1). NSGCTs comprised testicular epidermoid cyst (TEC, n = 6), mixed germ cell tumor (MGCT, n = 5), lymphomas (n = 3, 2 large B-cell lymphomas, 1 T-cell lymphoma), a yolk sac tumor (n = 1), a Leydig cell tumor (n = 1), a mature teratoma (n = 1), an embryonal carcinoma (n = 1), and an immature teratoma (n = 1). The left testis was affected in 17 patients, and the right testis was affected in 21 patients. One case was invasive B-cell lymphoma that involved the left testis and the left and right epididymis.

MRI findings and statistical analysis are summarized in Table 2. Among the seminomas (n = 20), 19 tumors were composed of multiple nodules and had narrow obviously enhanced fibrovascular septa, and 1 tumor presented as a single 5.9 cm × 6.6 cm × 5.7 cm mass with no detectable septa (Fig. 2). No capsules or hemorrhagic or cystic degeneration were seen. The accuracy of MRI for preoperative diagnosis of seminoma was 95% (19/20). NSGCTs had a round or oval morphology. Hemorrhagic and cystic degeneration were common MRI manifestations (Figs. 3 and 4).

There were significant differences in the presence/absence of a capsule ($P = .001$), T1-weighted imaging (T1WI) signal intensity ($P = .047$), T2-weighted imaging (T2WI) signal intensity ($P < .001$), septa ($P < .001$), and hemorrhagic or cystic degeneration ($P < .001$) between seminomas and NSGCT.

## 4. Discussion

There are 2 main categories of testicular tumors, namely GCT and stromal tumors. GCT, which account for 95% of all

**Table 1**

**MRI parameters (Philips Ingenia 3.0T unit).**

| Sequence parameter | TSE-T2WI | TSE-T1WI | TSE-SPAIR | T1WI + CE | SPIR + CE |
|---|---|---|---|---|---|
| Plane | Transverse, sagittal | Transverse | Transverse | Transverse, sagittal | Sagittal |
| TE, ms | 100–120 | 8–10 | 70–90 | 8–10 | 10–12 |
| TR, ms | 5000–7000 | 500–700 | 3000–5000 | 500–700 | 550–600 |
| Echoes | 1 | 1 | 1 | 1 | 3/4 |
| FOV, mm | 200 × 200 | 180 × 180 | 150 × 150 | 180 × 180 | 200 × 200 |
| Slice thickness, mm | 3 | 3 | 3 | 3 | 3 |
| Gap, mm | 3.3 | 3.3 | 3.3 | 3.3 | 0.3 |
| Matrix, mm | 300–340 × 200–250 | 250–300 × 200–250 | 180–190 × 160–170 | 240–260 × 200–220 | 220–240 × 150–170 |
| NSA | 1 | 1 | 1 | 1 | 1.5 |
| WL | 1100–1200 | 1000–1100 | 700–800 | 1000–1100 | 500–600 |
| WW | 1900–2000 | 1700–1800 | 1200–1300 | 1700–1800 | 900–1000 |

CE = Gd-DTPA 0.2 mmol/kg, current speed 2.0 mL/s. CE = contrast enhancement, FOV = field of view, Gd-DTPA = gadolinium-diethylenetriaminepentaacetate, MRI = magnetic resonance imaging, NSA = number of signals average, SPAIR = spectral attenuated in-version recovery, SPIR = spectral presaturation with inversion recovery, T1WI = T1-weighted imaging, T2WI = T2-weighted imaging, TE = echo time, TR = repetition time, TSE = fast spin echo, WL = window level, WW = window width.

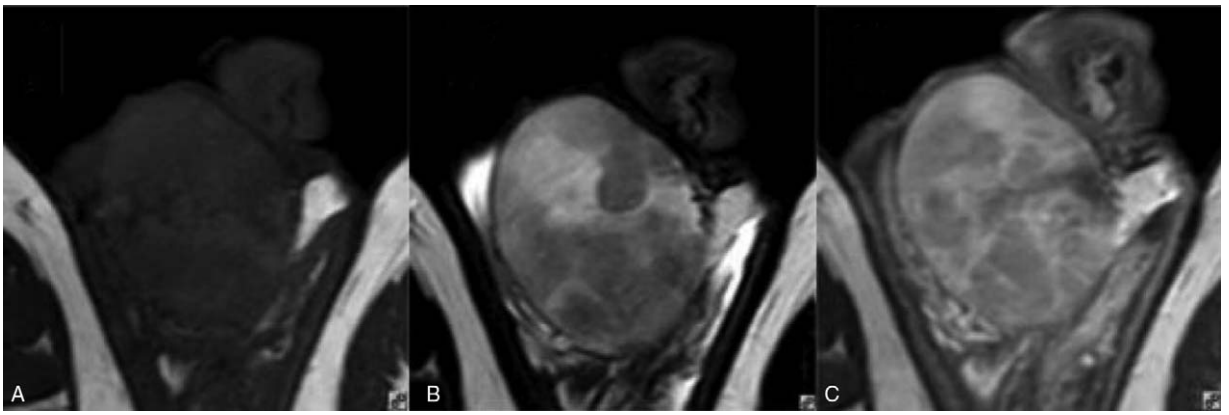


**Figure 1.** Thirty-three-year-old male with seminoma of the right testicle. (A) Transverse T1WI showing right testicular enlargement and an isointense signal; (B) transverse T2WI showing the tumor was formed by multiple hypointense nodules with isointense tissue between the nodules; and (C) transverse T1WI + CE showing the slim fibrous septa between the nodules was enhanced to the same extent as the internodal tissue. CE = contrast enhancement, T1WI = T1-weighted imaging, T2WI = T2-weighted imaging.

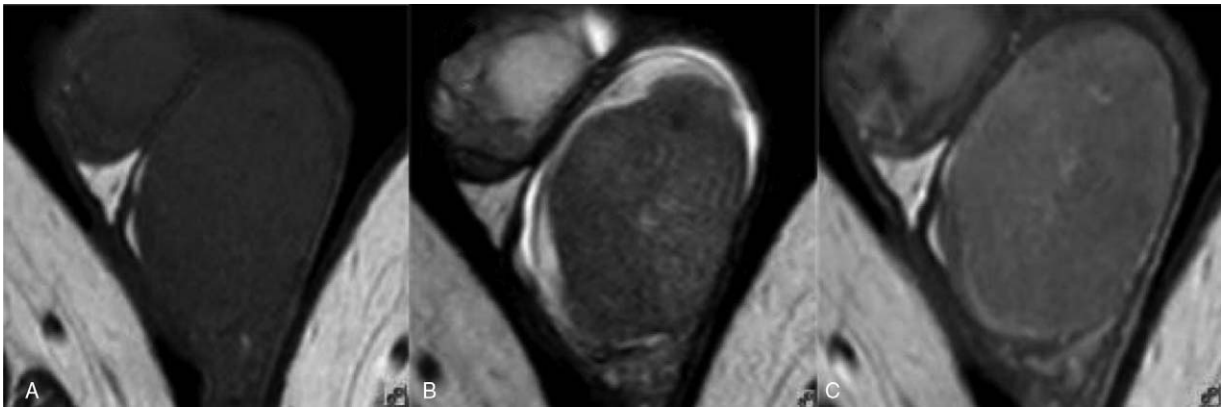


**Figure 2.** Forty-two-year-old male with seminoma of the left testicle. (A) Transverse T1WI showing left testicular enlargement and a uniform isointense signal; (B) transverse T2WI showing a hypointense tumor that comprised a single mass with shallow lobulation, the size of the tumor was 5.9 cm × 6.6 cm × 5.7 cm; and (C) transverse T1WI + CE showing a slightly enhanced tumor with no enhancement of the fibrous septa and an internal arterial blood supply. CE = contrast enhancement, T1WI = T1-weighted imaging, T2WI = T2-weighted imaging.

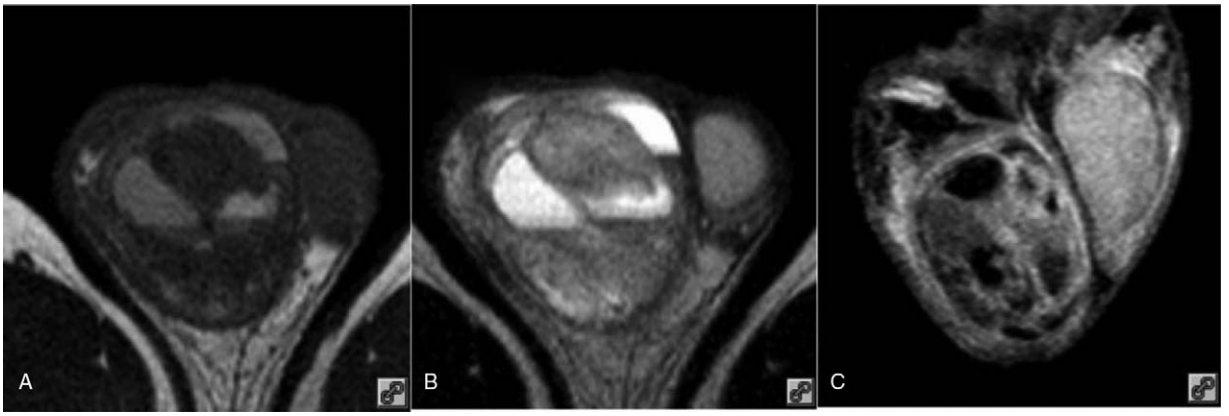


**Figure 3.** Thirty-two-year-old male with an MGCT. (A) Transverse T1WI showing the testicle was completely invaded by an oval shaped tumor. There was a mixed signal and a visible blood supply; (B) transverse T2WI showing a mixed signal; and (C) coronal SPIR + CE showing enhanced septa and a slightly enhanced tumor with cystic degeneration. CE = contrast enhancement, MGCT = mixed germ cell tumor, SPIR = spectral presaturation with inversion recovery, T1WI = T1-weighted imaging, T2WI = T2-weighted imaging.

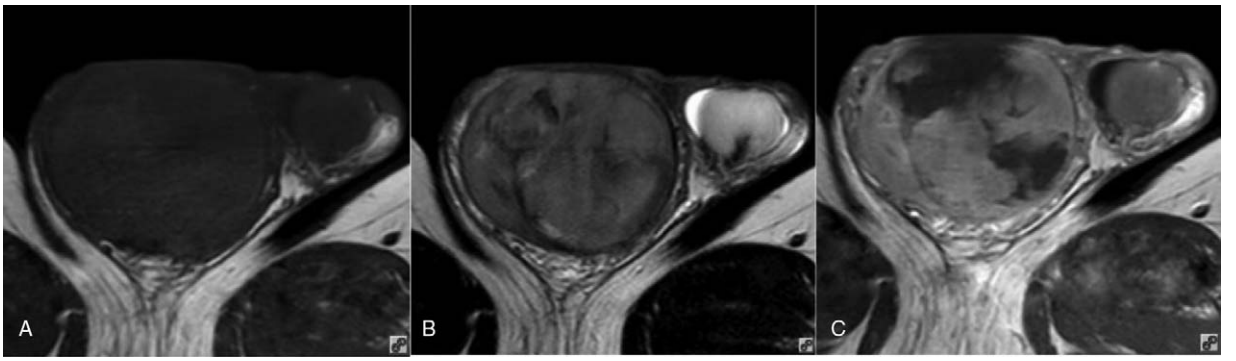


**Figure 4.** Fifty-six-year-old male with a large B-cell lymphoma. (A) Transverse T1WI showing a right testicular oval enlargement and an isointense signal; (B) transverse T2WI showing a hypointense signal; and (C) transverse T1WI + CE showing the septa were not enhanced. CE = contrast enhancement, T1WI = T1-weighted imaging, T2WI = T2-weighted imaging.

testicular tumors, is further subdivided into seminoma and NSGCT.[6] This subdivision is important for treatment purposes, as seminoma is highly radiosensitive, and NSGCTs respond better to a multimodal approach involving surgery and chemotherapy. MGCTs that contain seminomatous elements are treated as NSGCT. NSGCTs include embryonal carcinoma, lymphoma, choriocarcinoma, teratoma, yolk sac tumors, and other tumors. The histology of testicular tumors is age dependent: yolk sac tumors present in individuals aged 0 to 10 years, choriocarcinoma presents in individuals aged 20 to 30 years, embryonal carcinoma and teratoma present in individuals aged 25 to 30 years, and seminoma presents in individuals aged 30 to 40 years. Leydig cell tumor is the most common stromal tumor, and diffuse large B-cell type lymphoma is the most common primary testicular lymphoma (≥50 years old).[7]

US plays an important role in the evaluation of scrotal disease. MRI is not currently a front-line imaging modality for patients with acute scrotal disease, even though it allows acquisition of precise anatomic information, satisfactory tissue contrast, and imaging in various planes.[6] MRI does have utility for differential diagnosis, preoperative tumor staging, and can inform clinical decision-making. Specifically, MRI has value in the diagnosis of scrotal diseases with diverse etiologies, and for recognition of benign tumors such as TEC to avoid unnecessary radical orchiectomy.[8,9]

Diagnosis of testicular tumors on MRI requires a comprehensive analysis of morphology, presence or absence of a capsule, signal compared to the normal contralateral testicle, enhancement, septa, and hemorrhagic or cystic change. Findings from the present study suggest that tumor morphology on MRI facilitates differentiation of seminomas from NSGCTs. Most seminomas consisted of multiple nodules, while NSGCTs had a round or oval morphology. There were significant differences in the presence/absence of a capsule and presence of septa between seminomas and NSGCT. The mass, diameter, and volume of seminomas and NSGCTs measured and calculated from the transverse, sagittal plane of the MRI were not comparable. We propose that the morphological characteristics of seminomas are related to the polycentric development of the tumors. The septa within the tumor may be the residual testicular tissue, as they have a signal and enhancement that is similar to normal testicular tissue.

In our patients, seminomas appeared more homogeneous than NSGCT, isointense compared to normal testicular parenchyma on T1WI, and hypointense compared to spermatogenic cells on T2WI. Compared to NSGCT, seminomas did not demonstrate hemorrhagic or cystic change. There were significant differences in T1WI signal intensity, T2WI signal intensity, and hemorrhagic or cystic degeneration between seminomas and NSGCT. The hypointense signal on T2WI may reflect the density and lower water content of seminoma cells compared to normal spermatogenic cells.[10,11] Notably, hypointensity on T2WI is not sufficiently specific to make an accurate diagnosis of seminoma. Rather, seminomas may be characterized by the presence of hypointense bandlike structures on T2WI that are obviously enhanced, which represents a network of fibrovascular septa.[12]

In the present study, hemorrhagic and cystic degeneration were common MRI manifestations of NSGCT, which caused heterogeneously mixed signals on T1WI and T2WI. The hemorrhagic and cystic degeneration may reflect the degree of malignancy of the tumor. NSGCTs comprised TECs, MGCTs, lymphomas, a yolk sac tumor, a Leydig cell tumor, a mature teratoma, an embryonal carcinoma, and an immature teratoma. The 3 lymphomas were isointense on T1WI and hypointense on T2WI, with mild enhancement, which is consistent with previous reports.[13,14] The hypointense signal on T2WI may reflect the reduced cytoplasm and low water content of lymphoma cells compared to normal spermatogenic cells. Morphologically, lymphoma can be divided into diffuse and nodular types.[15] Among our patients, 1 large B-cell lymphoma had no enhancement of fibrous septa within the tumor and obvious cystic degeneration. Another large B-cell lymphoma was of interest because the tumor involved the left testis and the left and right epididymis. Testicular lymphoma is common in patients over 50 years old[7]; therefore, patient age can assist in differential diagnosis.

Yolk sac tumor is a highly malignant tumor that originates from the endoderm.[16] The tumors have mixed signals on T1WI and T2WI as they are composed of a multitude of morphological patterns, including microcystic, glandular, endodermal sinus-like, and myxomal, accompanied by hemorrhagic and cystic degeneration. Septa are hypointense on T2WI with significant enhancement after contrast administration. Yolk sac tumors may be differentiated from seminomas on MRI as the septa appears irregular and varies in thickness.

In our study, a Leydig cell tumor presented as a mixed signal on T1WI and a hypointense signal on T2WI, likely due to tumor hemorrhage. This case showed significant and continuous enhancement after contrast administration, which is consistent with published literature.[17,18]

**Table 2**

**MRI of testicular tumors (n = 39).**

| Group | | NSGCT (n = 19) | | | | | | | | *P |
|---|---|---|---|---|---|---|---|---|---|---|
| Item | Seminoma (n = 20) | TEC (n = 6) | MGCT (n = 5) | Lymphoma (n = 3) | Yolk sac tumor (n = 1) | Leydig cell tumor (n = 1) | Embryonal carcinoma (n = 1) | Mature teratoma (n = 1) | Immature teratoma (n = 1) | |
| Size†, cm/bulk, $cm^3$ | MN: 1–25 mm (n = 19); A single briquette: 116.16 $cm^3$ (n = 1) | Mean 25.62 $cm^3$ | Mean 31.46 $cm^3$ | Mean 51.06 $cm^3$ | 53.13 $cm^3$ | 2.68 $cm^3$ | 49.64 $cm^3$ | 14.91 $cm^3$ | 5.12 $cm^3$ | – |
| Capsule | No (n = 20) | Yes (n = 6) | No (n = 5) | No (n = 3) | No (n = 1) | No (n = 1) | No (n = 1) | Yes (n = 1) | Yes (n = 1) | .001 |
| T1WI | Isointense (n = 20) | Mixed (n = 6) | Mixed (n = 5) | Isointense (n = 3) | Mixed (n = 1) | Mixed (n = 1) | Mixed (n = 1) | Mixed (n = 1) | Mixed (n = 1) | .047 |
| T2WI | Hypointense (n = 20) | Mixed (n = 6) | Mixed (n = 5) | Hypointense (n = 3). | Mixed (n = 1) | Hypointense (n = 1) | Mixed (n = 1). | Hyperintense (n = 1) | Mixed (n = 1) | <.001 |
| Septa | Yes (n = 19) No (n = 1) | No (n = 6) | No (n = 4) Yes (n = 1) | No (n = 2) Yes (n = 1) | Yes (n = 1) | No (n = 1) | No (n = 1) | No (n = 1) | No (n = 1) | <.001 |
| HCD | No (n = 20) | No (n = 6) | Yes (n = 4) | Yes (n = 3) | Yes (n = 1) | Yes (n = 1) | Yes (n = 1) | No (n = 1) | No (n = 1) | <.001 |
| AFP | (–) | (–) | (+) (n = 5) | (–) | (+) | (–) | (+) | (–) | (–) | – |
| β-HCG | (+) (n = 1) | (–) | (+) (n = 5) | (–) | (+) | (–) | (+) | (– | (–) | – |
| ILN | (+) (n = 1) | (–) | (+) (n = 1) | (–) | (+) | (–) | (–) | (– | (–) | – |
| RLN | (+) (n = 1) | (–) | (–) | (–) | (–) | (–) | (+) | (– | (–) | – |
| Diagnosis | Seminoma (n = 19), lymphoma (n = 1) | Testicular epidermoid cyst (n = 5), benign uncertain (n = 1) | Uncertain (n = 5) | Lymphoma (n = 2), seminoma (n = 1) | Malignancy uncertain (n = 1) | Leydig cell tumor (n = 1) | Malignancy uncertain (n = 1) | Mature teratoma (n = 1) | Immature teratoma (n = 1) | – |

β-HCG, the normal range <2.6 IU/L; AFP, the normal range 0 to 9 ng/mL, AFP = alpha fetoprotein, HCD = hemorrhage or cystic degeneration, β-HCG = human chorionic gonadotropin, ILN = inguinal lymph node, MGCT = mixed germ cell tumor, MN = multiple nodules, MRI = magnetic resonance imaging, NSGCT = nonseminomatous germ cell tumor, RLN = retroperitoneal lymph node, TEC = testicular epidermoid cyst.

* Statistical analysis: Stata 12.0, Chi-square or Fisher, $P < .05$ was statistically significant.

† Three diameters were measured on the sagittal plane of the MRI (a: length, b: width, and c: depth), V (bulk) = 1/6, π, (a × b × c).

In addition to MRI findings, we reported on the immunohistochemical characteristics of the testicular tumors included in this study. In NSGCTs, alpha fetoprotein (AFP) elevation was seen in the yolk sac tumor and MGCTs but in very few teratomas, and increased human chorionic gonadotropin (β-HCG) was seen in the choriocarcinomas. In the seminomas, AFP levels were within normal range in all cases (normal 0−ng/mL), and β-HCG was elevated in 1 case. These data imply that the increase in AFP and β-HCG in the yolk sac tumor, MGCT, and embryonic carcinoma may be helpful for the differential diagnosis of seminoma before surgery.

In the present study, 2 cases of seminoma and 3 cases of NSGCT developed inguinal lymph node and retroperitoneal lymph node metastases. Previous reports suggest that all NSGCTs except choriocarcinoma show early metastasis to the retroperitoneal lymph nodes, and an estimated 30% of Stage I NSGCT are accompanied by retroperitoneal lymph nodes with micrometastases at diagnosis.[19] These data indicate that whole-abdominal computed tomography (CT) scanning should be performed when testicular malignancy is detected by MRI. The accuracy of CT for the diagnosis of lymph node metastases associated with testicular tumors is 89%[20]; therefore, whole-abdominal CT scanning plays an important role in the diagnosis, prognosis, and follow-up of testicular tumors.

According to preoperative MRI of the testicular tumors in this study, specific diagnostic criteria for seminoma are an isointense signal on T1WI, a hypointense signal on T2WI, and the presence of hypointense fibrovascular septa on T2WI that are obviously enhanced. Accuracy of preoperative MRI for diagnosis of seminomas based on these criteria was 95.00% (19/20). Preoperative MRI may not accurately identify MGCTs, yolk sac tumors, or embryonal carcinomas that have hemorrhagic and cystic degeneration but no specific tissue components, such as fat or fiber. The benign TEC could not be clearly distinguished from a benign cystic teratoma as there was no typical onion skin sign or bull's-eye sign on MRI.[8,9]

This study was associated with several imitations. First, testicular tumor is a rare disease, and the small number of samples in this study may lead to biased results. Second, the pathological basis of the hypointense signal on T2WI as a feature associated with testicular disease needs to be further studied as it may be related to the blood−testis barrier or a result of an infectious lesion in the testis.

In conclusion, this study of the MRI manifestations of testicular tumors suggests that preoperative MRI can distinguish seminoma from NSGCT. We propose that preoperative MRI of the scrotum is an effective technique that should be widely adopted for the management of scrotal disease.

## Author contributions

**Conceptualization:** Renwei Liu.
**Data curation:** Renwei Liu.
**Formal analysis:** Renwei Liu.
**Investigation:** Renwei Liu.
**Methodology:** Renwei Liu.
**Project administration:** Renwei Liu.
**Resources:** Zhengxian Lei.
**Software:** Aibo Li.
**Supervision:** Yixiang Jiang.
**Validation:** Jiayin Ji.
**Writing – original draft:** Renwei Liu.
**Writing – review & editing:** Renwei Liu.

## References

[1] Chia VM, Quraishi SM, Devesa SS, et al. International trends in the incidence of testicular cancer, 1973−2002. Cancer Epidemiol Biomarkers Prev 2010;19:1151–9.
[2] Dogra VS, Gottlieb RH, Oka M, et al. Sonography of the scrotum. Radiology 2003;227:18–36.
[3] Shtricker A, Silver D, Sorin E, et al. The value of testicular ultrasound in the prediction of the type and size of testicular tumors. Int Braz J Urol 2015;41:655–60.
[4] Tsili AC, Argyropoulou MI, Giannakis D, et al. Diffusion-weighted MR imaging of normal and abnormal scrotum: preliminary results. Asian J Androl 2012;14:649–54.
[5] Kim W, Rosen MA, Langer JE, et al. US MR imaging correlation in pathologic conditions of the scrotum. Radiographics 2007;27:1239–53.
[6] Woodward PJ, Sohaey R, O'Donoghue MJ, et al. From the archives of the AFIP: tumors and tumorlike lesions of the testis: radiologic-pathologic correlation. Radiographics 2002;22:189–216.
[7] Doll DC, Weiss RB. Malignant lymphoma of the testis. Am J Med 1986;81:515–24.
[8] Liu R, Lei Z, Chen N, et al. Imaging in testicular epidermoid cysts. Clin Imaging 2018;50:211–5.
[9] Cho JH, Chang JC, Park BH, et al. Sonographic and MR imaging findings of testicular epidermoid cysts. AJR Am J Roentgenol 2002;178:743–8.
[10] Mustafa F, Price E. Atlas of Tumor Pathology: Tumors of the Male Genital System. Vol 8, Ser 2. Washington, DC: Armed Forces Institute of Pathology; 1973. 7−84.
[11] Pretorius E, Siegelman E. MRI of the Male Pelvis and Bladder. Body MRI Philadelphia, PA: Elsevier Saunders; 2005. 372−386.
[12] Ueno T, Tanaka YO, Nagata M, et al. Spectrum of germ cell tumors: from head to toe. Radiographics 2004;24:387–404.
[13] Nagatsuma K, Tanomogi H, Hasegawa S, et al. [A case of malignant lymphoma of the testis: characterization with ultrasonography and magnetic resonance imaging]. Hinyokika Kiyo 1999;45:645–7.
[14] Saito W, Amanuma M, Tanaka J, et al. A case of testicular malignant lymphoma with extension to the epididymis and spermatic cord. Magn Reson Med Sci 2002;1:59–63.
[15] Tartar VM, Trambert MA, Balsara ZN, et al. Tubular ectasia of the testicle: sonographic and MR imaging appearance. AJR Am J Roentgenol 1993;160:539–42.
[16] Monig SP, Schmidt R, Krug B. Yolk sac tumor of the anterior mediastinum: the role of palliative surgery. Am Surg 1997;63:948–50.
[17] Fernandez GC, Tardaguila F, Rivas C, et al. Case report: MRI in the diagnosis of testicular Leydig cell tumour. Br J Radiol 2004;77:521–4.
[18] Zhu J, Luan Y, Li H. Management of testicular Leydig cell tumor: a case report. Medicine (Baltimore) 2018;97:e11158.
[19] Huddart RA, Birtle AJ. Recent advances in the treatment of testicular cancer. Expert Rev Anticancer Ther 2005;5:123–38.
[20] Moerman C. CT scan and testis tumors. J Belge Radiol 1993;76:82–3.